Journal of Biomechanics 84 (2019) 211–217

Contents lists available at ScienceDirect

Journal of Biomechanics

journal homepage: www.elsevier.com/locate/jbiomech
www.JBiomech.com

A fully nonlinear viscohyperelastic model for the brain tissue applicable to dynamic rates

Aref Samadi-Dooki, George Z. Voyiadjis *

Computational Solid Mechanics Laboratory, Department of Civil and Environmental Engineering, Louisiana State University, Baton Rouge, LA 70803, USA

ARTICLE INFO

Article history:
Accepted 2 January 2019

Keywords:
Brain biomechanics
Traumatic brain injury
Impact loading condition
Viscohyperelastic model
Nonlinear mechanical behavior

ABSTRACT

Understanding the mechanical response of the brain to external loadings is of critical importance in investigating the pathological conditions of this tissue during injurious conditions. Such injurious loadings may occur at high rates, for example among others, during road traffic or sport accidents, falls, or due to explosions. Hence, investigating the injury mechanism and design of protective devices for the brain requires constitutive modeling of this tissue at such rates. Accordingly, this paper is aimed at critically investigating the physical background for viscohyperelastic modeling of the brain tissue with scrutinizing the elastic fields pertinent to large, time dependent deformations, and developing a fully nonlinear multimode Maxwell model that can mathematically explain such deformations. The proposed model can be calibrated using the simple monotonic uniaxial deformation of the sample extracted from the tissue, and does not require additional information from relaxation or creep experiments. The performance of the proposed model is examined using the experimental results of two different studies, which reveals a desirable agreement. The usefulness, limitations, and future developments of the proposed model are discussed in this paper.

1. Introduction

Brain tissue is arguably the most vulnerable organ during accidents and traumatic conditions that involve impact or blast loading conditions. Such high-rate loadings can cause acute subdural hematoma, brain contusion, and diffuse axonal injury, the pathological conditions which, in general, are termed as traumatic brain injuries (TBIs) (Faul et al., 2010). To attain a better understanding of the mechanisms involved in a mild or severe TBI, researchers have utilized computer simulation as a powerful tool to estimate the forces and displacements generated in the tissue during injurious accidents, and compare them with the damage criteria at micro and macro scales (Ahmadzadeh et al., 2014; Cloots et al., 2013; Kleiven, 2007; Prabhu et al., 2011). Validity and precision of such simulations, however, depend on the accuracy of the mechanical properties and constitutive models considered for the brain tissue, the intracranial interactions, and boundary conditions assumed during modeling.

Brain tissue is a highly nonlinear and heterogeneous material with a rate-dependent behavior (Jin et al., 2013; Kaster et al., 2011; MacManus et al., 2015; Miller, 2005; Miller and Chinzei, 2002; Pervin and Chen, 2009; Samadi-Dooki et al., 2017, 2018). Since TBI conditions usually involve high rate and large deformations, one needs to consider a nonlinear and rate dependent model for the brain to come up with meaningful results from simulations. The nonlinearity is usually handled with implementing hyperelastic models; accordingly, the deformation energy is presented as a function of strain and material dependent constants (Mihai et al., 2017; Moran et al., 2014; Ogden, 1997; Voyiadjis and Samadi-Dooki, 2018). Subsequently, the explicit stress-strain relations can be obtained by taking the partial derivatives of the energy function with respect to the strain (stretch) field, as will be described later in this paper. On the other hand, the viscous behavior is usually formulated *via* Prony series the constants of which are characterized by using the results of relaxation experiments (Budday et al., 2015; Miller and Chinzei, 1997; Prange and Margulies, 2002; Rashid et al., 2012). Nevertheless, such a methodology is more relevant to a linear behavior since the strain field pertinent to the viscous part is generally valid for a small deformation regime.

In this paper, a novel methodology is presented to formulate the large deformation of brain tissue at high rates with incorporating a unified strain field for both elastic and viscous behaviors. The proposed model is basically different from the previously developed

* Corresponding author.
E-mail addresses: asamad3@lsu.edu (A. Samadi-Dooki), voyiadjis@eng.lsu.edu (G.Z. Voyiadjis).

https://doi.org/10.1016/j.jbiomech.2019.01.007
0021-9290/

models in which the nonlinearity in elastic and viscous behaviors is implemented *via* nonlinear deformation dependent constants, and does not require information from different loading conditions. Accordingly, a generalized Maxwell model is developed which includes fully nonlinear springs and dashpots. To this end, the physical basis of a large deformation strain filed based on the Seth-Hill (Hill, 1968; Seth, 1961) approach is described. Next, the generalized solution for the stress-stretch relation of individual Maxwell elements for a monotonic constant rate deformation is presented. With such a closed-form solution, obtaining the numerical values for the model parameters due to the time-dependent behavior does not require information from relaxation experiments, and they can be found from the same monotonic ramp loading or unloading data which are used for characterizing the time-independent parameters. The appropriateness and accuracy of the model is studied *via* implementing it for formulating the compressive behavior of the brain tissue at rates pertinent to impact loading as compared with the experiments by Tamura et al. (2007) and Rashid et al. (2012). Lastly, the usefulness, limitations, and future developments of the proposed model are discussed.

2. Theory

2.1. Hyperelasticity and Seth-Hill class of strains

In general, the large deformation of nonlinear elastic solids is described by a strain energy function as:

$$\Psi = \Psi(I_1, I_2, I_3) \tag{1}$$

in which I_1, I_2, and I_3 are the first, second, and third invariants of the strain tensor, respectively. For soft tissues, in general, and the brain tissue, in particular, the Ogden hyperelastic energy function is usually used which is expressed as (Ogden, 1997):

$$\Psi_{Ogd} = \sum_{j=1}^{N} \left[\frac{2\mu_j}{m_j} I_1\left(\boldsymbol{E}^{(m_j)}\right) + \frac{1}{D_j}(J-1)^{2j} \right] \tag{2}$$

with μ_j, m_j, and D_j representing the material dependent constants as the shear modulus, degree of nonlinearity, and compressibility, respectively; J is the determinant of the deformation gradient, and $I_1\left(\boldsymbol{E}^{(m_j)}\right)$ represents the first invariant of the $m_j{}^{\text{th}}$ order Seth-Hill strain tensor $\boldsymbol{E}^{(m_j)}$. In addition, parameter N is the number of terms required to fit the material behavior. The m^{th} order material Seth-Hill strain tensor is defined as:

$$\boldsymbol{E}^{(m)} = \begin{cases} \frac{1}{m}(\boldsymbol{U}^m - \boldsymbol{I}), & m \neq 0 \\ ln(\boldsymbol{U}), & m = 0 \end{cases} \tag{3}$$

in which $\boldsymbol{U}$ is the right stretch tensor, and $\boldsymbol{I}$ is the 3×3 identity matrix. The principal components of the strain tensor (for both material and spatial descriptions) can be defined in terms of the principal stretches (λ_i's) as:

$$E_i^{(m)} = \begin{cases} \frac{1}{m}(\lambda_i^m - 1), & m \neq 0 \\ ln(\lambda_i), & m = 0 \end{cases} \tag{4}$$

with $i = 1, 2, 3$. To preserve the physical consistency of the deformation, factor m should attain a negative value for a compressive deformation and a positive value for a tensile deformation (see, e.g., Attard (2003), Attard and Hunt (2004), Moerman et al. (2016) and Voyiadjis and Samadi-Dooki (2018) for details and discussion). A hybrid definition with considering both positive and negative values of m may be considered for a general deformation field (Moerman et al., 2016).

The brain tissue can be considered to be mechanically incompressible, especially for a compressive deformation field (Voyiadjis and Samadi-Dooki, 2018), hence, the Ogden hyperelastic strain energy in terms of the principal stretches for this material may be presented as:

$$\Psi_{Ogd}(\lambda_1, \lambda_2, \lambda_3) = \sum_{j=1}^{N} \left[\frac{2\mu_j}{m_j^2} \left(\lambda_1^{m_j} + \lambda_2^{m_j} + \lambda_3^{m_j} - 3 \right) \right] \tag{5}$$

In addition, the principal Cauchy stresses (σ_i) for an incompressible material can be obtained from the energy function as:

$$\sigma_i = \lambda_i \frac{\partial \Psi}{\partial \lambda_i} - p, \quad i = 1, 2, 3 \tag{6}$$

in which p is the Lagrange multiplier and stands for the reaction hydrostatic pressure for incompressibility condition. Moreover, the deformation of an incompressible material satisfies the volume preserving condition as:

$$J = \lambda_1 \lambda_2 \lambda_3 = 1 \tag{7}$$

For an axial deformation (say, direction 1), considering the geometrical symmetry and the stress-free condition in lateral directions ($\sigma_2 = \sigma_3 = 0$), the relation between the axial stress σ and stretch λ can be obtained as:

$$\sigma = \sum_{j=1}^{N} \left[\frac{2\mu_j}{m_j} \left(\lambda^{m_j} - \lambda^{-m_j/2} \right) \right] \tag{8}$$

This equation may be rearranged as:

$$\sigma = \sum_{j=1}^{N} \left[\frac{2\mu_j}{m_j} (\lambda^{m_j} - 1) + \frac{\mu_j}{\frac{-m_j}{2}} \left(\lambda^{-m_j/2} - 1 \right) \right] \tag{9}$$

Considering Eq. (4) for the Seth-Hill principal strains, Eq. (9) can be further simplified as:

$$\sigma = \sum_{j=1}^{N} \left[\mu_j \left(2E^{(m_j)} + E^{(-m_j/2)} \right) \right] \tag{10}$$

with E representing the strain in the loading direction. Therefore, one may consider the part in the parentheses on the right hand side of Eq. (10) to present a hybrid strain as (Moerman et al., 2016):

$$\Xi^{(m)} = 2E^{(m)} + E^{(-m/2)} \tag{11}$$

Hence, the stress-strain relation for the axial deformation of an incompressible solid with an Ogden hyperelastic function reduces to:

$$\sigma_s = \sum_{j=1}^{N} \left[\mu_j \Xi_s^{(m_j)} \right] \tag{12}$$

The additional index s in this equation stands for the spring element in the viscoelastic solid. Interestingly, this equation resembles the classical stress-strain relation for linear elastic solids ($\sigma = E\epsilon$) but is valid for a large deformation nonlinear field with the aforementioned condition.

2.2. Nonlinear viscous behavior

To model the viscous part of the material behavior, the same definition for the nonlinear strain as the one obtained for the spring element is used herein. Accordingly, the stress-strain rate relation for the nonlinear dashpot element is obtained as:

$$\sigma_d = \sum_{j=1}^{N} \left[C_j \dot{\Xi}_d^{(m_j)} \right] \tag{13}$$

in which C_j is the dashpot constant, $\dot{\Xi}$ denotes the time derivative of the strain field, and index d is used to emphasize this relation corresponds to the dashpot element. With such a definition, one can be confident that both viscous and elastic fields are formulated based on the same nonlinear strain field which is an important requirement for consistency of the formalism for a large deformation.

2.3. Formalism for a fully nonlinear viscohyperelastic Maxwell model

One may now consider the generalized multimode Maxwell model for the monotonic deformation of the brain tissue as depicted in Fig. 1 which includes a nonlinear spring (for the long term behavior) in parallel with several Maxwell viscoelastic elements. While the overall stretch (strain) is the same for the left-most spring and the individual Maxwell elements, the overall stress is equal to the summation of stress in each branch as:

$$\sigma = \sum_{i=0}^{M} \sigma_i \tag{14}$$

in which M is the number of individual Maxwell elements and σ_0 is the stress in the left-most long-term elastic element.

While the stress-stretch relation for the long-term spring is described by Eq. (8), one requires obtaining such an explicit relation for the individual Maxwell elements. According to Fig. 1, the stress in the spring and dashpot of the i^{th} Maxwell elements are equal due to the fact that they are connected in series, hence:

$$\sigma_i = \sigma_{d_i} = \sigma_{s_i} \tag{15}$$

On the other hand, the strain in the i^{th} Maxwell element is equal to the summation of strain in the spring and dashpot elements, which for the aforementioned nonlinear strain field reads as follows:

$$\Xi_i = \Xi_{s_i} + \Xi_{d_i} \tag{16}$$

For modeling the tension-compression behavior of soft materials, an Ogden model with at least two terms is required. These terms should include positive and negative nonlinearity parameters for physical consistency (Attard, 2003; Kleiven, 2007; Voyiadjis and Samadi-Dooki, 2018). Nevertheless, for modeling sole tension or compression uniaxial deformation, an Ogden model with only one term is adequate to represent the material behavior (Budday et al., 2017; Voyiadjis and Samadi-Dooki, 2018). Hence, considering Eqs. (12) and (13) with $N = 1$ and Eqs. (15) and (16), the governing differential equation of the i^{th} Maxwell element is obtained as:

$$\dot{\Xi}^{(m_1^i)} = \frac{\dot{\sigma}_i}{\mu_1^i} + \frac{\sigma_i}{C_1^i} \tag{17}$$

or, in terms of the Seth-Hill strain as:

$$2\dot{E}^{(m_1^i)} + \dot{E}^{(m_1^i/2)} = \frac{\dot{\sigma}_i}{\mu_1^i} + \frac{\sigma_i}{C_1^i} \tag{18}$$

Combining Eq. (18) with Eqs. (10) and (14), one can describe the stress-strain (or stretch) relation for an axial deformation field in terms of the stretch (or stress) input as a function of time and material parameters m^i, μ^i, and C^i.

3. Results

3.1. Material characterization for a constant rate deformation field

For a constant stretch rate, the time dependent longitudinal stretch for a uniaxial deformation may be described as:

$$\lambda(t) = 1 + \alpha t \tag{19}$$

in which α is a constant that determines the rate of deformation and is positive or negative for a tensile or compressive deformation, respectively. For such a stretch field as the input, the stress *vs* time relation for the i^{th} Maxwell element in Fig. 1 is obtained as:

$$\begin{aligned}\sigma^i(t) = \mu_1^i e^{-\frac{1+\alpha t}{\alpha\tau_1^i}} \Bigg(& 2\Pi_{1-m_1^i}\left(-\frac{1}{\alpha\tau_1^i}\right) + \Pi_{\frac{m_1^i}{2}+1}\left(-\frac{1}{\alpha\tau_1^i}\right) \\ & - 2(1+\alpha t)^{m_1^i}\Pi_{1-m_1^i}\left(-\frac{1+\alpha t}{\alpha\tau_1^i}\right) \\ & - (1+\alpha t)^{-m_1^i/2}\Pi_{\frac{m_1^i}{2}+1}\left(-\frac{1+\alpha t}{\alpha\tau_1^i}\right)\Bigg)\end{aligned} \tag{20}$$

in which $\tau_1^i = \frac{C_1^i}{\mu_1^i}$ is the time constant for this element and $\Pi_n(z)$ is the exponential integral function defined as:

$$\Pi_n(z) = \int_1^{\infty} e^{-zt}/t^n dt \tag{21}$$

Accordingly, the overall stress *vs* time relation of the nonlinear multimode Maxwell solid of Fig. 1 for a uniaxial deformation at a constant stretch rate reads as:

$$\begin{aligned}\sigma(t) = & \frac{2\mu_1^0}{m_1^0}\left((1+\alpha t)^{m_1^0} - (1+\alpha t)^{-m_1^0/2}\right) \\ & + \sum_{i=1}^{M}\mu_1^i e^{-\frac{1+\alpha t}{\alpha\tau_1^i}}\Bigg(2\Pi_{1-m_1^i}\left(-\frac{1}{\alpha\tau_1^i}\right) \\ & + \Pi_{\frac{m_1^i}{2}+1}\left(-\frac{1}{\alpha\tau_1^i}\right) - 2(1+\alpha t)^{m_1^i}\Pi_{1-m_1^i}\left(-\frac{1+\alpha t}{\alpha\tau_1^i}\right) \\ & - (1+\alpha t)^{-m_1^i/2}\Pi_{\frac{m_1^i}{2}+1}\left(-\frac{1+\alpha t}{\alpha\tau_1^i}\right)\Bigg)\end{aligned} \tag{22}$$

In practice, usually the engineering (first Piola-Kirchhoff) stress is obtained from the experiments which is defined as the load divided by the original cross section area of the element. For the case of uniaxial testing of an incompressible material, the principal engineering stress in the loading direction (P_1) may be obtained from the Cauchy stress as (Holzapfel, 2000):

$$P_1 = \frac{\sigma_1}{\lambda_1} \tag{23}$$

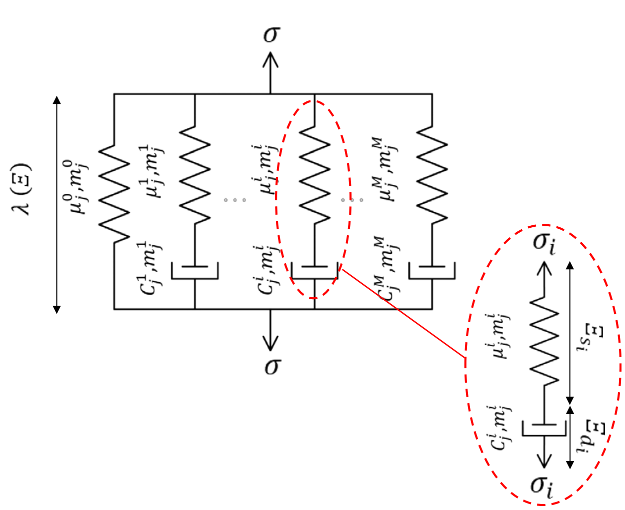

Fig. 1. Schematic representation of the proposed nonlinear multimode Maxwell model.

3.2. Model validation and parameter identification

Using Eqs. (22) and (23) one can obtain the model constants from the input stress *vs* time data for a uniaxial deformation at a constant rate. In this study, the experiments by Tamura et al. (2007) and Rashid et al. (2012) are used for validating the proposed model. In both of the aforementioned studies, the large deformation response of the tissue during high-rate unconfined compression is investigated. While Tamura and coworkers obtained the response of the white matter for compressive deformation up to 50% engineering strain at rates of 1, 10, and 50 s^{-1}, Rashid et al. performed their experiments on samples of mixed white and gray matters for strains up to 30% and rates of 30, 60, and 90 s^{-1} (see Fig. 2).

To validate the proposed model, it is first calibrated using the result of the two aforementioned studies for their respective highest rates. Accordingly, the stress *vs* time data for these rates is extracted using Eqs. (22) and (23) and the FindFit function of Mathematica 11.3 (Wolfram Research Inc., Champaign, IL) with a maximum of 2000 iterations. The model is implemented using a Maxwell model with three elements only as shown in Fig. 3a which results in one time constant for the model (additional terms can be considered for more complex loading modes or different rates). In addition, the nonlinearity parameter is assumed to be equal for all elements in each model for each experiment and attain a negative value due to the compressive nature of the load. The numerical values for each experimental study are obtained as presented in Table 1 and the results based on the model and the experiments are shown in Fig. 3b and c for the selected rates.

The results of the previous step are used for obtaining the stress-strain curves for the other two rates in each study and compared with the experimentally obtained values as demonstrated in

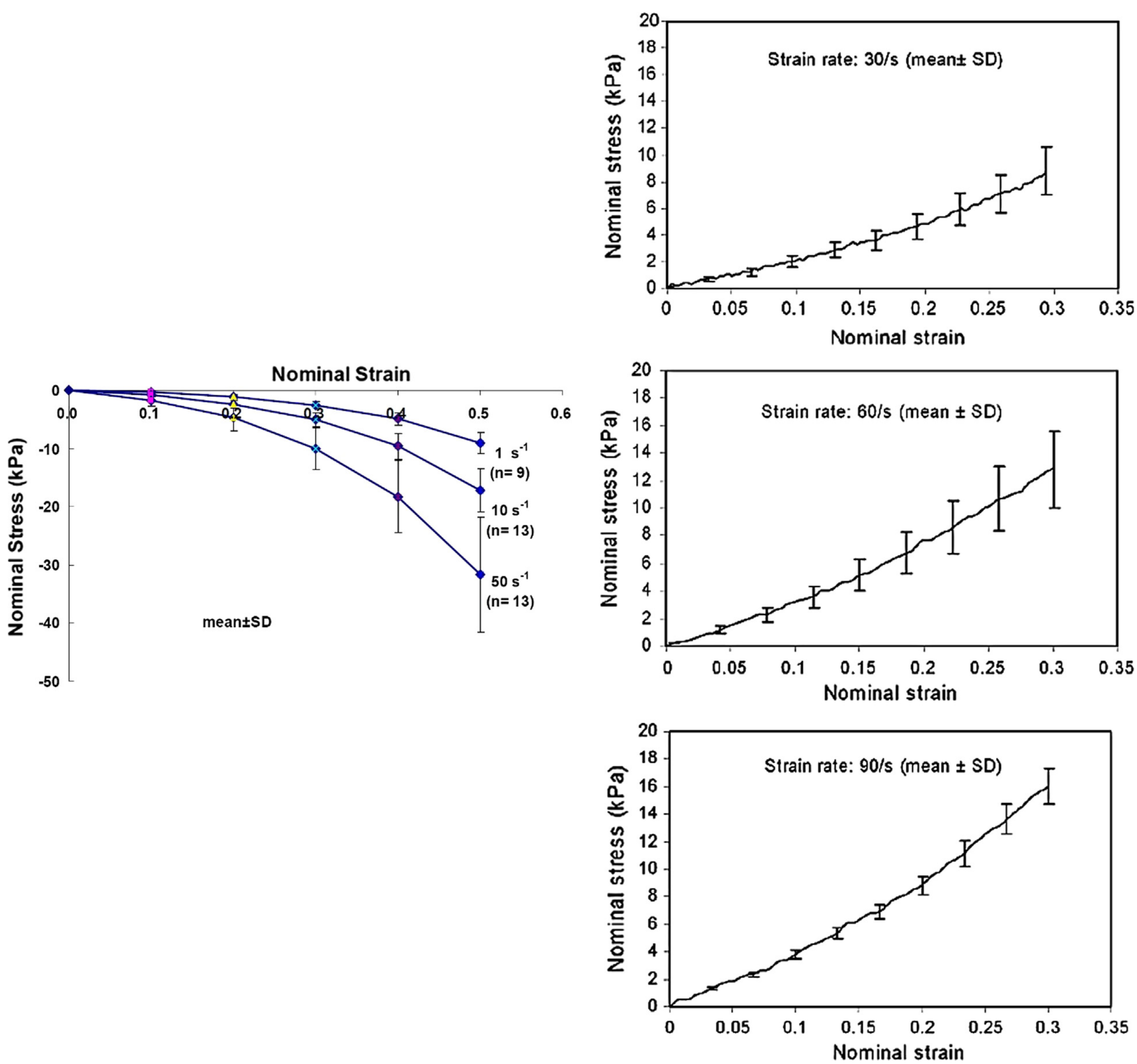

Fig. 2. The stress *vs* strain for unconfined compression of the brain tissue at dynamic rates based on the experiments performed by left: Tamura et al. (2007), and right: Rashid et al. (2012) (reproduced with permissions from the Japan Society of Mechanical Engineers and Elsevier, respectively).

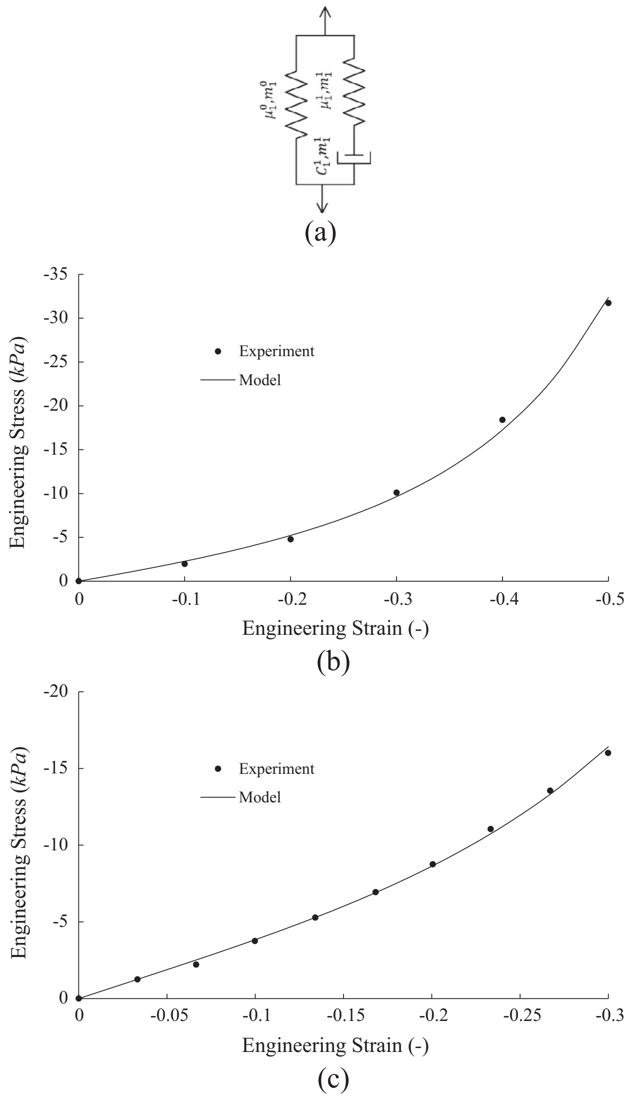

Fig. 3. (a) The nonlinear Maxwell model utilized for estimating the dynamic behavior of the brain tissue; (b) fitting the proposed model based on the experiments by Tamura et al. (2007) at the compressive strain rate of 50 s^{-1}; (c) fitting the proposed model based on the experiments by Rashid et al. (2012) at the compressive strain rate of 90 s^{-1}. The numerical values for model parameters based on the fitting are presented in Table 1.

Fig. 4, which exhibit an excellent performance for the proposed model.

4. Discussion

4.1. Unifying the strain definition for nonlinear elastic and viscous elements

To mathematically explain the nonlinear large deformation and rate dependent behavior of soft materials, viscohyperelastic models are usually used for modeling and FE simulation purposes. The nonlinear elastic part in such formalisms is expressed in terms of either hyperelastic energy functions which incorporate higher order strains, or nonlinear elastic constants which are functions of deformation. The viscous part, on the other hand, is formulated based on either the time-dependent relaxation behavior, or incorporating nonlinear dashpot constants which are functions of deformation rate. It is, however, important to note that use of hyperelastic energy functions implies incorporating a certain definition for the strain field during large deformation (Voyiadjis and Samadi-Dooki, 2018). On the other hand, explaining the rate dependent part of the deformation in terms of relaxation functions may not take into account the same definition for the strain field. Such a formalism, hence, results in a physically inconsistent constitutive model for the overall behavior for a material with viscoelastic behavior. For example, for a Maxwell model, the differences in the definition of the strain field for the spring and dashpot elements, which are connected in series, causes an incorrect combination of the overall strain as obtained by summation of the strains in the two parts. For a Kelvin model in which the strains in the dashpot and spring elements are assumed to be equal, the difference in definition of the strain for the two parts violates the equality of stretches.

In this paper, the main effort is to unify the strain field for the nonlinear spring and dashpot elements in the viscoelastic solid that is used for investigating the high-rate large deformation behavior of the brain tissue. This approach is basically different from the aforementioned procedures for modeling this phenomenon. In classical approaches for defining a nonlinear dashpot element, the stress is related to the strain rate with higher order polynomial functions (such as $\sigma = E\dot{\epsilon}^n$) or a nonlinear dashpot constant is used. In the current study, however, a novel approach for formulating the nonlinear behavior of the dashpot element is proposed which relies on replacing the classical strain rate with the rate of the nonlinear Seth-Hill strain as shown in Eq. (13). This approach not only unifies the strain field for the nonlinear dashpot and spring elements, but also results in a closed-form solution for the deformation of the material that can be calibrated based on single monotonic uniaxial loading. In addition, the formalism can be easily established for other loading conditions such as simple shear or biaxial loadings.

4.2. Response of the brain tissue at dynamic rates

The novel model presented herein is suitable for formulating the behavior of the brain tissue at rates pertinent to impact or blast loading conditions. Accordingly, the material parameters can be obtained for one rate and used for other rates without requiring the information from relaxation or creep experiments. For modeling the large deformation-rate dependent behavior of the brain, some researchers have excluded the dashpot element and obtained constants of the hyperelastic model (shear moduli and nonlinearity constants) for different rates (see, e.g., Begonia et al. (2010) and Rashid et al. (2012)). Such an approach not only implies that the strain energy (free energy) function is rate dependent which is inconsistent with the principal of thermodynamics (Truesdell and Noll, 2004), but also results in model parameters which are only useful for certain rates.

Comparing the results based on two different experimental studies for the porcine brain tissue, the modeling process suggests

Table 1
Numerical values for the model parameters of the nonlinear Maxwell model with three elements.

Based on the experiments by:	m_1^0 and $m_1^1(-)$	μ_1^0 (Pa)	μ_1^1 (Pa)	τ_1^1 (ms)	R^2
Tamura et al. (2007)	−2	1100	34.3	5.83	0.9970
Rashid et al. (2012)	−3	799	24	2.04	0.9986

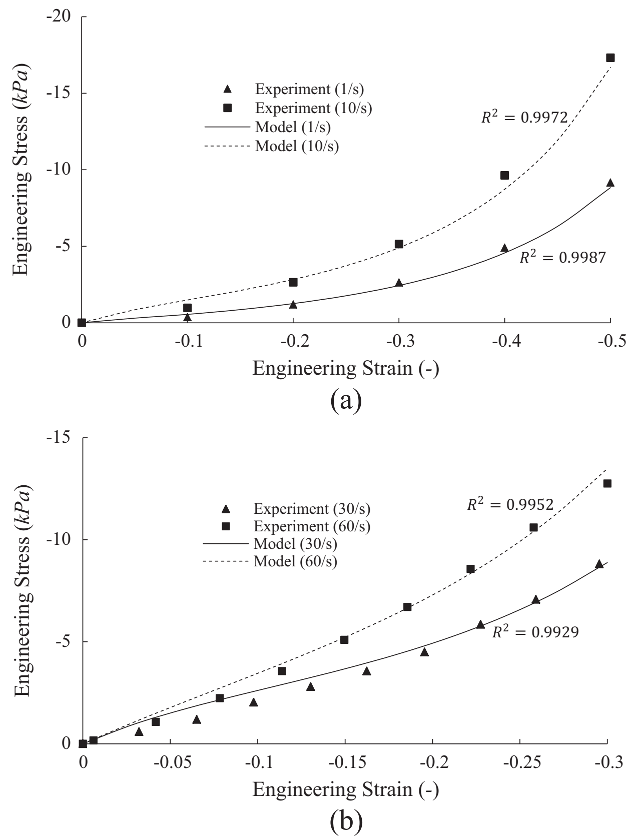

Fig. 4. Examining the performance of the proposed model with the numerical values presneted in Table 1 as obtained for the highest rates for two different experiments. The stress-strain curves for the slower rates are obtained and compared with the experiments of (a) Tamura et al. (2007), and (b) Rashid et al. (2012).

the white matter is slightly stiffer than the mixed white and gray matters (see Table 1). This observation is in agreement with several studies reporting the stiffer response of the white matter compared to the gray matter (Budday et al., 2015; Pervin and Chen, 2009; Samadi-Dooki et al., 2017) but is not a general conclusion since there exist some studies in which stiffer behavior of the gray matter compared to the white matter is reported (Budday et al, 2017; Prange and Margulies, 2002). In addition, the time constant obtained for the individual Maxwell element for both set of experiments is in the order of milliseconds, which is within the same range as the loading duration in impact condition.

4.3. Limitations and future developments

Although the proposed model exhibits superior performance in describing the high-rate large-deformation of the brain, it is built upon some simplifying assumptions. Firstly, an isotropic mechanical behavior is assumed for the brain tissue. It is well-known that the brain (especially the white matter) consists of fiber bundles that can cause directional dependent mechanical response of the tissue. Nevertheless, recent studies have shown that such fiber orientation induced anisotropies are not of statistical significant (Budday et al., 2017; Giordano et al., 2014), hence, the results of the model can be extended to a general 3D deformation. In addition, to reduce the mathematical complexities, a single-term Ogden energy function is used in this study. Although even a one-term Ogden model has been shown to suffice for modeling the uniaxial deformation of the brain (Budday et al., 2017; Voyiadjis and Samadi-Dooki, 2018), the fact that multiple Maxwell elements can be considered in the model according to Eq. (22) brings about the same effect as increasing the terms in the energy function.

To be applicable to the full-scale mechanical investigation of the brain, the model needs to be used in finite element (FE) simulations. Nevertheless, the equations for such a constitutive model do not exist in the library of commercial FE packages. Hence, the future development of this model includes developing subroutines that can be incorporated in FE software for large-scale modeling of the brain at high rates.

5. Conclusion

Understanding the response of the brain to its mechanical environment is of critical importance for studying the pathological conditions of this tissue during traumatic injuries. Since most of the circumstances that result in TBI involve high-rate loading conditions, constitutive modeling of the biomechanics of the brain at such elevated rates is required for computer simulations that aimed at predicting the onset of injury and its localization. Accordingly, the current model offers a physically based approach for modeling the high-rate-large-deformation of the brain with developing a fully nonlinear multimode Maxwell solid. The model exhibits excellent agreement with unconfined compressive deformation of the brain, and the findings can be used for studying the behavior of this tissue at rates relevant to the impact or blast loading conditions.

6. Conflict of interest statement

The authors declare that there are no conflicts of interest associated with this work.

References

Ahmadzadeh, H., Smith, D.H., Shenoy, V.B., 2014. Viscoelasticity of tau proteins leads to strain rate-dependent breaking of microtubules during axonal stretch injury: predictions from a mathematical model. Biophys. J. 106, 1123–1133.
Attard, M.M., 2003. Finite strain––isotropic hyperelasticity. Int. J. Solids Struct. 40, 4353–4378.
Attard, M.M., Hunt, G.W., 2004. Hyperelastic constitutive modeling under finite strain. Int. J. Solids Struct. 41, 5327–5350.
Begonia, M.T., Prabhu, R., Liao, J., Horstemeyer, M.F., Williams, L.N., 2010. The influence of strain rate dependency on the structure–property relations of porcine brain. Ann. Biomed. Eng. 38, 3043–3057.
Budday, S., Nay, R., de Rooij, R., Steinmann, P., Wyrobek, T., Ovaert, T.C., Kuhl, E., 2015. Mechanical properties of gray and white matter brain tissue by indentation. J. Mech. Behav. Biomed. Mater. 46, 318–330.
Budday, S., Sommer, G., Birkl, C., Langkammer, C., Haybaeck, J., Kohnert, J., Bauer, M., Paulsen, F., Steinmann, P., Kuhl, E., 2017. Mechanical characterization of human brain tissue. Acta Biomaterialia 48, 319–340.
Cloots, R.J., Van Dommelen, J., Kleiven, S., Geers, M., 2013. Multi-scale mechanics of traumatic brain injury: predicting axonal strains from head loads. Biomech. Model. Mechanobiol. 12, 137–150.
Faul, M., Xu, L., Wald, M.M., Coronado, V.G., 2010. Traumatic brain injury in the United States. Atlanta, GA: Centers for Disease Control and Prevention, National Center for Injury Prevention and Control.
Giordano, C., Cloots, R., Van Dommelen, J., Kleiven, S., 2014. The influence of anisotropy on brain injury prediction. J. Biomech. 47, 1052–1059.
Hill, R., 1968. On constitutive inequalities for simple materials—I. J. Mech. Phys. Solids 16, 229–242.
Holzapfel, A.G., 2000. Nonlinear Solid Mechanics: A Continuum Approach for Engineering. John Wiley & Sons, Chichester.
Jin, X., Zhu, F., Mao, H., Shen, M., Yang, K.H., 2013. A comprehensive experimental study on material properties of human brain tissue. J. Biomech. 46, 2795–2801.
Kaster, T., Sack, I., Samani, A., 2011. Measurement of the hyperelastic properties of ex vivo brain tissue slices. J. Biomech. 44, 1158–1163.
Kleiven, S., 2007. Predictors for traumatic brain injuries evaluated through accident reconstructions. Stapp. Car. Crash. J. 51, 1–35.
MacManus, D., Pierrat, B., Murphy, J.G., Gilchrist, M., 2015. Dynamic mechanical properties of murine brain tissue using micro-indentation. J. Biomech. 48, 3213–3218.
Mihai, L.A., Budday, S., Holzapfel, G.A., Kuhl, E., Goriely, A., 2017. A family of hyperelastic models for human brain tissue. J. Mech. Phys. Solids 106, 60–79.

Miller, K., 2005. Method of testing very soft biological tissues in compression. J. Biomech. 38, 153–158.
Miller, K., Chinzei, K., 1997. Constitutive modelling of brain tissue: experiment and theory. J. Biomech. 30, 1115–1121.
Miller, K., Chinzei, K., 2002. Mechanical properties of brain tissue in tension. J. Biomech. 35, 483–490.
Moerman, K.M., Simms, C.K., Nagel, T., 2016. Control of tension–compression asymmetry in Ogden hyperelasticity with application to soft tissue modelling. J. Mech. Behav. Biomed. Mater. 56, 218–228.
Moran, R., Smith, J.H., García, J.J., 2014. Fitted hyperelastic parameters for Human brain tissue from reported tension, compression, and shear tests. J. Biomech. 47, 3762–3766.
Ogden, R.W., 1997. Non-linear Elastic Deformations. Courier Corporation.
Pervin, F., Chen, W.W., 2009. Dynamic mechanical response of bovine gray matter and white matter brain tissues under compression. J. Biomech. 42, 731–735.
Prabhu, R., Horstemeyer, M., Tucker, M., Marin, E., Bouvard, J., Sherburn, J., Liao, J., Williams, L.N., 2011. Coupled experiment/finite element analysis on the mechanical response of porcine brain under high strain rates. J. Mech. Behav. Biomed. Mater. 4, 1067–1080.
Prange, M.T., Margulies, S.S., 2002. Regional, directional, and age-dependent properties of the brain undergoing large deformation. J. Biomech. Eng. 124, 244–252.
Rashid, B., Destrade, M., Gilchrist, M.D., 2012. Mechanical characterization of brain tissue in compression at dynamic strain rates. J. Mech. Behav. Biomed. Mater. 10, 23–38.
Samadi-Dooki, A., Voyiadjis, G.Z., Stout, R.W., 2017. An indirect indentation method for evaluating the linear viscoelastic properties of the brain tissue. J. Biomech. Eng. 139, 061007.
Samadi-Dooki, A., Voyiadjis, G.Z., Stout, R.W., 2018. A combined experimental, modeling, and computational approach to interpret the viscoelastic response of the white matter brain tissue during indentation. J. Mech. Behav. Biomed. Mater. 77, 24–33.
Seth, B., 1961. Generalized Strain Measure with Applications to Physical Problems. MRC Technical Summary Report #248. Mathematics Research Center, United States Army, University of Wisconsin, pp. 1–18.
Tamura, A., Hayashi, S., Watanabe, I., Nagayama, K., Matsumoto, T., 2007. Mechanical characterization of brain tissue in high-rate compression. J. Biomech. Sci. Eng. 2, 115–126.
Truesdell, C., Noll, W., 2004. The Non-linear Field Theories of Mechanics. Springer, Berlin.
Voyiadjis, G.Z., Samadi-Dooki, A., 2018. Hyperelastic modeling of the human brain tissue: effects of no-slip boundary condition and compressibility on the uniaxial deformation. J. Mech. Behav. Biomed. Mater. 83, 63–78.